Science of the Total Environment 814 (2022) 152572

Contents lists available at ScienceDirect

Science of the Total Environment

journal homepage: www.elsevier.com/locate/scitotenv

Kinetics of microplastic generation from different types of mulch films in agricultural soil

Yang Yang [a,1], Zhen Li [a,b,1], Changrong Yan [a,b], Dave Chadwick [c,d], Davey L. Jones [c,d], Enke Liu [a], Qin Liu [a,b], Runhao Bai [a], Wenqing He [a,b,*]

[a] Institute of Environment and Sustainable Development in Agriculture, Chinese Academy of Agricultural Sciences, Beijing 100081, PR China
[b] Key Laboratory of Prevention and Control of Residual Pollution in Agricultural Film, Ministry of Agriculture and Rural Affairs, Beijing 100081, PR China
[c] School of Natural Sciences, Bangor University, Bangor, Gwynedd LL57 2UW, UK
[d] SoilsWest, UWA School of Agriculture and Environment, The University of Western Australia, Perth, WA 6009, Australia

HIGHLIGHTS

- Kinetics of microplastic generation from mulch films were studied upon UV irradiation.
- Biodegradable films were most rapid in microplastic formation, followed by oxo-film and PE film.
- Kinetics of microplastic generation strictly followed the Schwarzchild's law.
- Crystallinity and chemical composition are critical for the size and quantity of microplastics.
- At cumulative UV exposure of 2.1 MJ/m^2, 147–475 microparticles/cm^2 could be released.

GRAPHICAL ABSTRACT

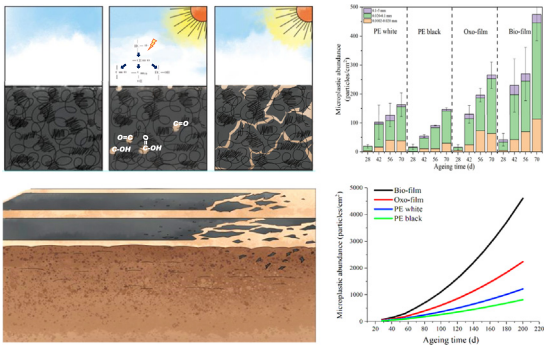

ARTICLE INFO

Article history:
Received 23 August 2021
Received in revised form 16 December 2021
Accepted 16 December 2021
Available online 23 December 2021

Editor: Jay Gan

Keywords:
Mulch film
Microplastic generation
UV irradiation
Emission kinetics
Schwarzchild's principle

ABSTRACT

Upon environmental weathering, plastic materials form smaller sized microplastics, of which the contamination in agricultural fields is of significant importance and increasing social concern. Plastic mulch films are considered a major source of agricultural soil microplastic pollution. However, the mechanism and kinetics of microplastic formation from plastic mulch films were rarely understood. In this study, the rate of microplastic generation from typical mulch films, such as oxodegradable, biodegradable, and conventional non-degradable (polyethylene, PE) mulch films, were quantified in soil under simulated UV irradiation. Results showed that microplastic formation was more rapid from biodegradable mulch film, followed sequentially by oxodegradable mulch film, white PE mulch film, and black PE mulch film. The kinetics of microplastic generation strictly followed the Schwarzchild's law, with exponential growth at indexes between 1.6309 and 2.0502 in the microplastic generation model. At a cumulative UV irradiation of 2.1 MJ/m^2, the average quantity of microplastics released from biodegradable, oxodegradable, and white and black non-degradable mulch films were 475, 266, 163, 147 particles/cm^2, respectively; with particle sizes largely distributed within 0.02–0.10 mm range. Concurrent increase in crystallinity and surface erosion of the mulch films were observed upon UV irradiation, which further determined the accessibility and activity of the materials to photo-oxidation (reflected as HI indexes), therefore played a critical role on the quantity and size ranges of microplastic debris.

* Corresponding author at: Institute of Environment and Sustainable Development in Agriculture, Chinese Academy of Agricultural Sciences, Beijing 100081, PR China.
E-mail addresses: yangyang05@caas.cn (Y. Yang), lizhen@caas.cn (Z. Li), hewenqing@caas.cn (W. He).
[1] These authors contributed equally to this work and should be considered as co-first authors.

http://dx.doi.org/10.1016/j.scitotenv.2021.152572

1. Introduction

Large application and release of plastics into the environment is increasingly recognized as a serious environmental issue worldwide (Horton et al., 2017; MacLeod et al., 2021). Once in the environment, plastic undergoes abiotic and biotic degradation, thereby causing gradual fragmentation and generation of smaller sized particles, those of which less than 5 mm-diameter are termed as microplastics (Thompson et al., 2009). Eriksen et al. (2014) estimated that 6.25×10^4 microparticles at approximately 0.80 mm diameter can be generated from each piece of plastic with a diameter of 200 mm and thickness of 0.20 mm. Because of the small particle sizes, microplastics can easily penetrate and accumulate in living organisms (Bhagat et al., 2020; Li et al., 2020), thereby negatively affecting the health, growth, and reproduction of plant and animals (Ding et al., 2021; Qi et al., 2018) or even migrate and accumulate through the food chain, hence causing health risks to humans (Huerta Lwanga et al., 2017; Lehner et al., 2019) and resulting in significantly greater contamination hazard than macroplastic debris. However, early studies on microplastics mainly focused on aquatic ecosystems, leaving a large knowledge gap on their impacts to terrestrial ecosystems, especially agricultural systems (de Souza Machado et al., 2019; Rillig, 2012), which is surprising because most plastics in freshwater and marine systems originated on land (He et al., 2018; Stubbins et al., 2021). Deep investigations on the terrestrial and farmland microplastic pollution are of urgent and significant importance.

Plastic film mulching is now one of the most important agricultural technologies in China, with the annual coverage area reaching approximately 18 million hm^2 and the annual quantity usage surpassing 1.45 million tons (China Agriculture Yearbook, 2019; Sun et al., 2020). However, the ubiquitous and repeated application of mulch films resulted in increasing quantities of plastic film residuals in the agricultural and horticultural fields (Gao et al., 2019; Liu et al., 2014), as mulch films deteriorate and fragment during the growing season and are very difficult to be fully recollected from the soil. Up to 25%–33% of total mulching input could remain in the field each year (Yan et al., 2015; Li et al., 2018). Nowadays, for the intensive mulching areas in China, the average quantity of mulch film residues in soil ranged between 50 and 270 kg/hm^2 with the highest concentrations of 265.3–381.1 kg/hm^2 found in cotton fields in Xinjiang, >100 kg/hm^2 in Gansu and Inner Mongolia, and <80 kg/hm^2 in the soils of North and Southwest of China (Qi et al., 2020; Yan et al., 2015). As a huge source of microplastic contamination in agriculture soil, this large amount of macro-sized plastic mulch film residuals is alarming but has not been given enough attention before (MacLeod et al., 2021; Rillig et al., 2017; Steinmetz et al., 2016). Biodegradable and oxodegradable mulch films were developed to reduce the persistence of macroplastic pollution compared with conventional non-degradable mulch films and are now occupying an increasing share of the mulch film market, especially in China. However, their use is inevitable for releasing microplastic (Briassoulis et al., 2015a; Briassoulis et al., 2015b; Cai et al., 2018; Laycock et al., 2017; Rudnik and Briassoulis, 2011; Zhang et al., 2021). Studies have reported the increased levels of microplastic in mulched fields compared with non-mulched fields (Huang et al., 2020; Zhou et al., 2020), thereby highlighting the importance of mulch films on microplastic formation. However, the quantitative contribution of plastic mulch film to soil microplastic contamination, specifically the rate and kinetics of microplastic formation from different types of mulch films, has not been explored.

Ultraviolet (UV) radiation by inducing peroxidation and molecular chain scission is generally acknowledged as the most important degradation factor and rate limiting process for plastic breakdown in outdoor environments (Albertsson and Hakkarainen, 2017; Ammala et al., 2011; Laycock et al., 2017; Uheida et al., 2021; Zhang et al., 2021). This phenomenon is particularly true for mulch films, which are high molecular weight polymers with high hydrophobicity and semi-crystalline structures to provide the properties needed for tensile strength and minimizing evaporation, hence are hardly available to the actions of microorganisms, especially in the early deterioration stage (Kasirajan and Ngouajio, 2012; Li et al., 2019). By UV irradiation attacks, the molecular bond of CC and CH breaks up, generates highly active free radicals that can readily react with oxygen, produces carbonyl or hydroxyl acids, and eventually leads to the scission and crosslinking of molecular chains following the Norrish I and/or Norrish II degradation reactions (Ammala et al., 2011). The photochemical induced brittleness by random chain scission and crosslinking of plastic polymers may subsequently result in the formation of small plastic particles from large plastic debris (Julienne et al., 2019; Qi et al., 2020). The morphological changes (i.e., holes and cracks on the surface of the deteriorated materials) indicate the degrees of environmental weathering (Cai et al., 2018; Iniguez et al., 2018); whereas the presence and intensity of carbonyl and hydroxyl functional groups are widely used to characterize the photo oxidation reactivity of the plastic materials (Chen et al., 2021; Fairbrother et al., 2019).

Apart from the particular chemical reactions and various appearances of plastic aging, such as the changes in surface morphology, formation of oxidation products, and fragmentations, the most basic and fundamental mechanism underlying the UV oxidation processes is the breakage of molecular bonds by energetic UV photons (with energies greater than that of molecular covalent bond) and thus the formation of reactive free radicals (Ammala et al., 2011; Fairbrother et al., 2019; Li et al., 2019). Therefore, a dose-dependent relationship would be expected for the UV aging phenomenon, such that the degree of degradation increases with the level of UV irradiation (Bigger et al., 1992; Hsu et al., 2012; Martin et al., 2003). For a quantitative understanding of the photo oxidation processes, numerous efforts have been devoted by numerous scientists and researchers. One of the most representative studies is conducted by Sommersall and Guillet, who aimed to develop a numerical model for polyolefin photooxidation by considering all of the possible elementary chemical steps (Somersall and Guillet, 1985). This study is of significant importance, however, the chemical steps are largely oversized (up to sixty) for most oxidation cases, and the rate constant of most of the steps are experimentally out-of-reach. For a less precise but simplified understanding of the process, Bunsen and Roscoe conducted the first reciprocity experiments, from which they concluded that the outcome of a photochemical reaction depends dominantly on the total absorbed energy of photo irradiation (Martin et al., 2003). This is later known as the reciprocity law, which is expressed as $It = constant$, where I is the radiant intensity, and t is the exposure time (Martin et al., 2003). On this basis, a more generalized mathematical equation has later been established, known as the Schwarzchild's law, which is expressed as $It^p = \text{constant}$. I is the irradiance intensity, t is the exposure time, and p is the coefficient factor that varies for different materials and irradiance ranges (Croll, 2019; Martin et al., 2003). The Schwarzchild's law is proven excellent at interpreting and predicting dose-damage relationship of photooxidation exposure, such as chemical changes, yellowish coloring, or decreases in mechanical strength during plastic deterioration (Diepens and Gijsman, 2009; Martin et al., 2003). As microplastics result from macromolecular chain scissions that are largely controlled by UV irradiate oxidations (Zhu et al., 2020), it is highly attractive for deep investigations on whether microplastic formation from plastic mulch films upon UV irradiation following the Schwarzchild's principle.

In this study, we selected the major types of commercial mulch films, including conventional non-degradable, oxodegradable, and biodegradable mulch films, for investigation. Our main aims were to (i) quantify the generation of microplastics from mulch films in agricultural soil when exposed to UV radiation; (ii) explore the mechanism underlying the behavior and kinetics of microplastics generation; and (iii) compare the potential environmental burdens of microplastic emissions from different types of mulch films used in agriculture. These results are critical for understanding the kinetics and mechanisms of microplastic generation from agricultural mulch films, which are key for comparing the wider agronomic and environmental impacts of different types of mulch films.

2. Materials and methods

2.1. Materials

Four typical types of commercial mulch films at the thickness of 0.08 mm were bought from agricultural suppliers. Detailed information on the physical properties of mulch films were presented in Table S1. The major content of the biodegradable mulch film was determined by FTIR as polybutyrate adipate terephthalate (PBAT). For the three other types of mulch films (e.g., oxodegradable mulch film, conventional white mulch film, and conventional black mulch film), the major component was verified as polyethylene (PE) (Fig. S2).

Soil was collected from the experimental base of the Chinese Academy of Agricultural Sciences in Shunyi district, Beijing, at the depth of 0–10 cm. The soil is loamy brown, previously cultivated of maize, with averaged organic matter content at 23.7 g/kg, and pH value of 8.0. Prior to use, the soil was rinsed 2 times in excessive quantity of Milli-Q water to wash out the suspended microplastic and other impurities. Then, the soil was air-dried, sieved through 2 mm mesh, and watered to 40% of total water-holding capacity according to the instructions of EN 17033: 2018 Annex A and ISO 11274. The pH was adjusted to 8.0 in reference to ISO 10390. The organic matter content showed slight decrease to 20.0 g/kg after the pretreatment.

2.2. Aging experiments

The four types of mulch film samples were cut into 1 cm^2, placed in separate glass dishes, and buried in between 3.5 g (0.5 cm in thickness) of the pretreated soil with less than 0.10 cm of soil upon the pieces of mulch films and 0.40 cm of soil under beneath. This 0.10 cm of soil above the pieces of mulch films were used to keep the film residuals in place during the experiment and to avoid potential cross contaminations between the treatments. This also resembles the realistic situation of mulch film application in field, when a thin layer of soil was usually intentionally laid upon the films as to keep it in place against the wind. Also, for film residuals that are not fully recollected from the fields, it is very often that these residuals were under beneath of thin layers of soil (Fig. S1).

The different treatments were then placed in weathering chamber (BGD 866, Biuged, China) (Fig. 1). Accelerated weathering procedures were performed in accordance to ISO 4892-2. The weathering chamber is equipped with xenon-arc lamp and daylight filter that provides continuous irradiation at spectral range of 320–400 nm at irradiance level of approximately 0.35 W/m^2, thereby simulating the irradiance of natural summer solar light in the North of China (Zhu et al., 2021). The UV intensity (at spectral range of 320–400 nm) at the surface and 0.10 cm depth of soil are monitored with a spectrometer (AvaSpec-2048-USB2), at the rate of 31.52 μmol·m^{-2}·s^{-1} and 8.10 μmol·m^{-2}·s^{-1}, respectively.

The relative humidity of the chamber is controlled at 65%, by 18 mins' spray of deionized water mist after each 102 min interval. Mulch samples were taken at the 28th, 42nd, 56th, and 70th day of UV radiation. Three replicates were established for each type of mulch film samples at each time point in parallel with a series of non-mulch film controls (soil only) to account for any potential interferences from other potential microplastic contaminations.

2.3. Mulch film characterization

Fourier transform infrared (FTIR) spectrometer (LUMOS, Bruker Optik GmbH, Germany) was used to monitor the chemical changes in surface functional groups. Due to the heterogeneous surface texture of weathered plastic films, spectra were measured at three different surface regions for each sample at a wavelength range of 400–4000 cm^{-1}, resolution of 4 cm^{-1}, and 32 scans for each site. All the spectra were further processed by automatic baseline correction. The hydroxyl index (HI) values were calculated by taking the ratio of hydroxyl absorbance at 3600 cm^{-1} to 3100 cm^{-1} to the absorbance of the CH stretching at 1472 cm^{-1} that remains unchanged during oxidation. The surface morphology of the aged films were investigated via scanning electron microscopy (SEM) (SU-8010, Hitachi, Japan) at 20 kV electron accelerating voltage.

To calculate the crystallization ratio of specific surface areas, the X-ray diffraction (XRD) was performed using an advance diffractometer (D8, Bruker, USA) equipped with a Cu Kα radiation source (λ = 0.154 nm) and a Hi-Star general area diffraction detection system for 2D images in a 2θ range from 5 to 80°. The crystallization ratio was calculated as Eq. (1) in reference to Li et al. (2014):

$$Crystallinity\ (\%) = \frac{\sum_{i=1}^{n} A_{ci}}{A_t} \times 100\%, \quad (1)$$

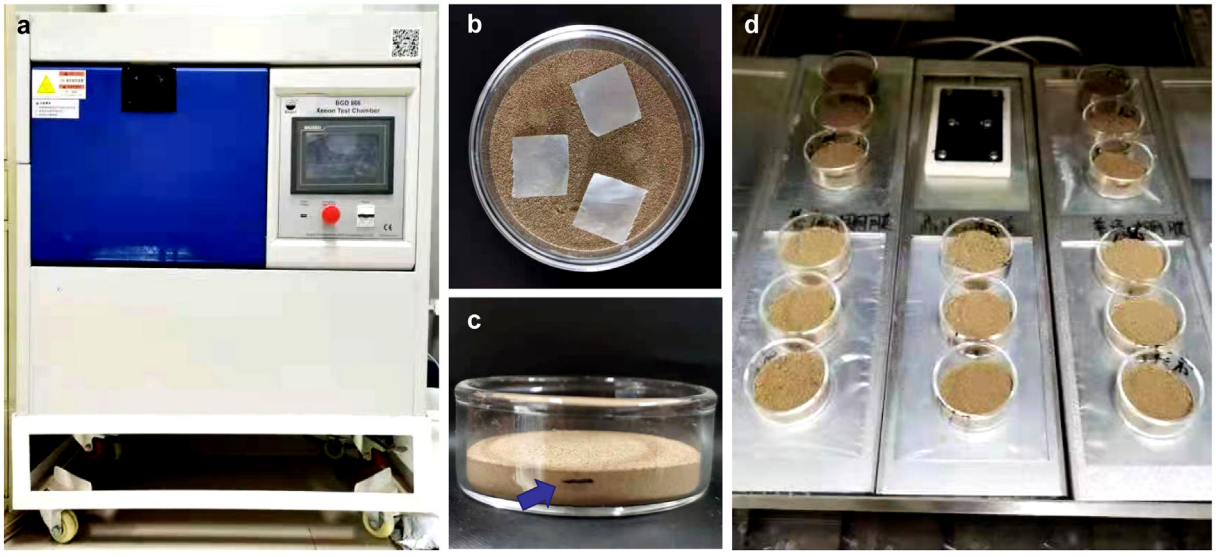

Fig. 1. Aging experiment. (a) Photograph of the weathering chamber (BGD 866, Biuged, China); (b) distribution of mulch film pieces inside the glass dishes (three pieces of the same mulch film sample were placed in one glass dish); (c) the localization of the film pieces in the glass dishes, the black line marks the localization of mulch film pieces, with 1.0 mm of soil on top and 4.0 mm of soil in below; (d) three replicates of glass dishes were established for each of the four types of mulch film samples at each time point in parallel with a series of non-mulch film control (soil only). The UV intensity (at spectral range of 320–400 nm) at the surface and at a soil depth of 0.10 cm are 31.52 μmol·m^{-2}·s^{-1} and 8.10 μmol·m^{-2}·s^{-1}, respectively.

where A_{ci} is the area of crystalline peak i, and A_t is the total area of the crystalline peak and amorphous background in the diffractogram.

2.4. Microplastic sampling

A modified density separation method with saturated sodium iodide solution (1.85 g/cm^3) was used to extract and quantify the microplastics released from deteriorated mulch films to soil samples in reference to Liu et al. (2018). Briefly, soil from each incubation vessels were transferred into a 100 mL glass beaker with 70 mL of saturated NaI solution and agitated with a magnetic stirrer for 30 min before being allowed to settle for 12 h. The supernatants were carefully decanted to clean glass beakers through flotation. The magnetic stirring and flotation steps for each treatment were repeated three times to ensure the full extraction of microplastics. The supernatants of each treatment were transferred into a 250 mL glass beaker, and 100 mL of 30% H_2O_2 were added to digest the organic matters for 12 h. This purification reaction system was kept at low temperature in ice water bath. The digested solution was filtered through a 7 μm glass fiber filter and then stained with Nile Red fluorescence solution for 30 min before vacuum filtration through 0.2 μm glass fiber filters. The filters with microplastics were dried at room temperature and stored in separate glass dishes. The size and amount of microplastics on each filter were recorded using a fluorescent stereomicroscope (LEICA M165 FC, Germany) within 24 h. The quantity and size distribution of the microplastic were analyzed using Image J software. The polymer composition of the collected microplastics were further verified with a FTIR microscope (LUMOS I, Bruker Optik GmbH, Germany).

2.5. Kinetic modeling

For quantitative expression of the dose-dependent damages by UV photooxidation, the Schwarzchild's formula, which is expressed as in Eq. (2), has been introduced:

$$It^p = constant, \tag{2}$$

where I is the irradiance intensity, t is the exposure time, and p is the coefficient factor that varies for different materials and irradiance ranges (Croll, 2019; Martin et al., 2003).

It could also be expressed in Eq. (3) as:

$$k = BI^p, \tag{3}$$

where k is the degradation rate, and B is a coefficient.

These two equations are interchangeable, and the degradation rate k is inversely proportional to time t (Diepens and Gijsman, 2009).

A logarithm equation of Hahm–Kron is popularized for the graphical verification on the adaptability of the Schwarzschild's law, as expressed in Eq. (4):

$$\log It = constant + \log\left[\left(\frac{I}{I_0}\right)^a + \left(\frac{I}{I_0}\right)^{-a}\right], \tag{4}$$

where I_0 and ɑ are constants for specific photographic emulsions.

At low irradiance intensities, it can be simplified into Eq. (5) as:

$$\log It = constant - a \bullet \log I \tag{5}$$

If the Schwarzchild's law is obeyed, then a linear relationship should be obtained between the logarithm of photo response vs the logarithm of light intensity, and the slope of the line indicates the Schwarzschild p-coefficient factor (Lyu et al., 2018; Martin et al., 2003).

2.6. Statistical analysis

IBM SPSS 23.0 software was used for the statistical analysis, and a one-way analysis of variance (ANOVA) was selected for statistical testing (significance level = 0.05). Origin Pro 9.0 software and Sigmaplot 13.0 were used to perform data plotting and model fitting, respectively.

3. Results and discussion

3.1. Chemical degradation of mulch films

Photo-oxidation of plastic mulch films, including PE white mulch film, PE black mulch film and oxodegradable mulch film, were identified by FTIR spectrum with the presence and obviously increased vibration peaks of carbonyl (-C=O) and hydroxyl (-OH) groups at 1700–1800 cm^{-1} and 3324–3500 cm^{-1}, respectively (Fig. 2). For biodegradable mulch films, similar increased intensities of the -OH peak at 3324–3500 cm^{-1} were observed. Moreover, the absorption peak of the benzene rings at 1600–1450 cm^{-1} were significantly decreased (Fig. 2), thereby suggesting the breakup and degradation of benzene rings in PBAT molecular chains upon photo aging. The degradation of benzene rings of PBAT in agricultural soil have been proved by Zumstein et al. (2018) through ^{13}C-labeling on the different building blocks of PBAT and isotope-specific tracking of ^{13}C from biodegradable polymers into CO_2 and microbial biomass. As reported by Zumstein et al. (2018), although the degradation of terephthalate-rich domains on a PBAT surface was slower than that of the adipate rich domains, benzene rings could be degraded and mineralized in the soil.

Hydroxyl functional groups are major intermediate products of plastic photo oxidation and are widely applied as an indicator of photo oxidation reactivity. For a quantitative insight into the photo oxidation reactivity of the different mulch films, the changes in HI were monitored by using the area of the FTIR spectral hydroxyl band at 3600 cm^{-1} to 3100 cm^{-1}, normalized to the absorbance of CH stretching band at 1472 cm^{-1} that remains unchanged during oxidation (Table 1). Given the particularity of the functional groups of biodegradable mulch film and the lack of consistent reference absorption peaks in FTIR spectra, we only carried out HI analysis on the conventional and oxodegradable mulch films. As shown in Table 1, the oxodegradable mulch film responded fastest to photo irradiation, with HI sharply increasing from 0 to 1.272 in the first 28 days, which is 3–4 times higher than those of the PE white and PE black mulch films. However, after 42 days of photo irradiation, the HI values of PE black mulch films exceeded those of the oxodegradable mulch film and PE white mulch film at a ratio of 1.87 and 3.86, respectively. Moreover, with increased duration of UV irradiation from the 56th to 70th day, when the HI values for the oxodegradable mulch film and PE white mulch film decreased from 3.754 to 1.610 and 3.281 to 2.401, respectively; the PE black mulch film showed a continuous increase in HI from 3.429 to 4.231.

In reference to previous reports, the rapid increase in HI for oxodegradable mulch films in early deterioration phases could be due to the pro-oxidants contained in these mulch films, as pro-oxidants can largely accelerate the generation of free radicals and incorporation of oxygen, therefore accelerating the photo oxidation responses (Ammala et al., 2011; Zhao et al., 2006). In contrast, the different patterns of HI diagrams for the PE black mulch films may imply a contribution of carbon blacks, which are strong absorber of UV irradiation and efficient UV stabilizer, that may enhance the generation of hydroxyl radicals while blocking further Norrish II breakage reactions on macro-molecular chain by reversible proton transformation within the aromatic structures.

3.2. Morphology deterioration of plastic mulch film

The morphological changes in the surface of plastic mulch films were revealed by SEM images (Fig. 3). Before being exposed to UV irradiation, all the original mulch films showed a smooth and even surface; however, in the aged mulch films, different degrees of holes, cracks, and plaques were observed. Among all mulch film types, the biodegradable mulch film showed the roughest surface morphology after 70 days of UV irradiation and was fully covered with large cracks and plaques. In comparison, for the aged PE white mulch film, PE black mulch film, and oxodegradable

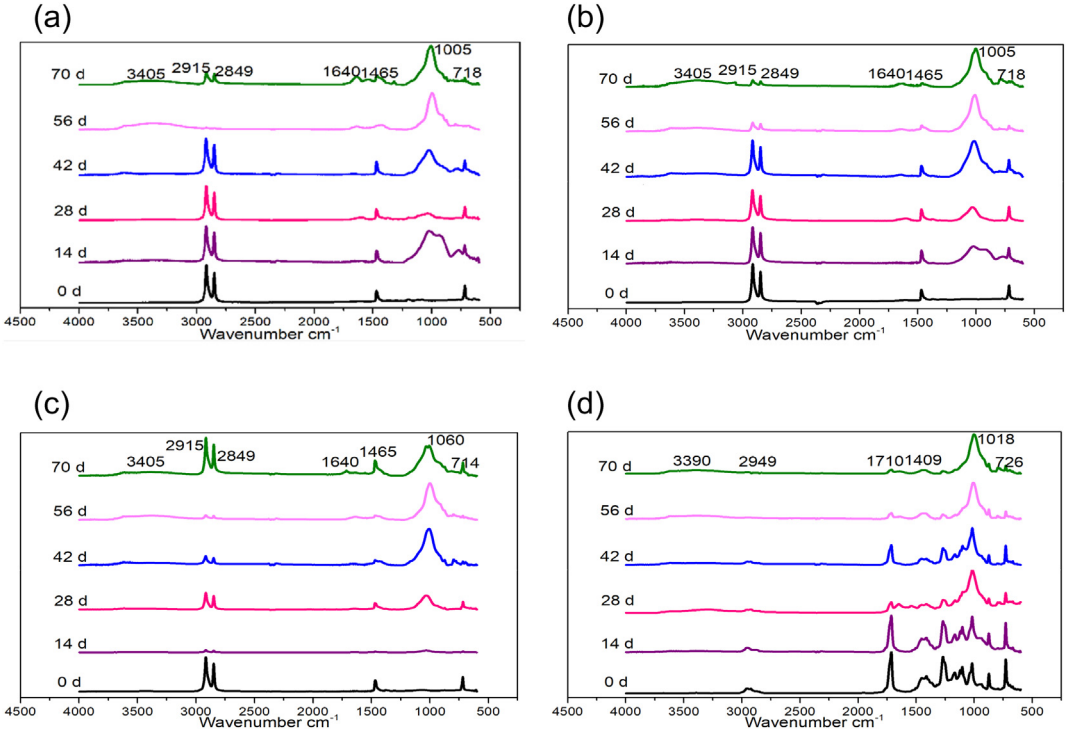

Fig. 2. FTIR spectra of mulch films at increasing periods (days) of UV exposure. (a) PE white, (b) PE black, (c) oxo degradable, and (d) biodegradable mulch films. The averaged UV intensity at the surface of the film debris is 8.10 μmol·m^{-2}·s^{-1}.

mulch films, only few cracks, holes, and small plaques were scattered on the surface. XRD investigations revealed an obvious increase in the surface crystallinity for the different types of mulch films after UV irradiation (Table 2). By 70 days of photooxidation, the crystallinity index of biodegradable mulch films had increased the most from 58.94 to 73.77 (at factor of 25.2%), and the oxodegradable mulch film increased from 26.79 to 32.84 (by 22.6%). The PE white and PE black mulch films were more moderate in elevation of crystallinity, at a ratio of 11.6% from 30.06 to 33.56 and 0.7% from 30.05 to 30.26, respectively.

Notably, molecular chain scissions primarily occurs in amorphous regions rather than in semi-crystalline or crystalline structures because of their higher accessibility (Julienne et al., 2019; Li et al., 2019), and considering the changes in chemical and morphological properties obtained by FTIR (oxidation reactivity), SEM, and XRD (crystallinity ratio) measurements in this study, it can be suggested that the visible changes in the surface microstructures of different types of mulch films were resulted by a series of chemical changes, including the removal of photooxidation by-products, restructuring of the surface amorphous content, and increased crystalline fractions that exceeded the regional tensile and formation of cracks and cavities on the mulch film surface (Julienne et al., 2019; Lambert and Wagner, 2016; Lyu et al., 2018; Zhang et al., 2021). The decreased HI values of PE white mulch film and oxodegradable mulch film during the 56th and 70th day of photodegradation may be largely due to the increased crystallinity and thus less accessibility of these materials to further degradation factors.

Table 1
Hydroxyl index of aged mulch film exposed to UV irradiation, n = 3.

Aging time	Hydroxyl index (μm)		
	PE white	PE black	Oxo-film
0 days	0.000	0.000	0.000
28 days	0.343 ± 0.141	0.425 ± 0.142	1.272 ± 0.436
42 days	0.606 ± 0.084	2.339 ± 1.814	1.245 ± 0.416
56 days	3.281 ± 2.841	3.429 ± 1.487	3.754 ± 2.574
70 days	2.401 ± 1.661	4.231 ± 4.534	1.610 ± 0.342

3.3. Generation of microplastics

The generation of microplastics was detected after 28 days of UV irradiation, and it increased with longer photo oxidation periods. Biodegradable mulch films had the highest rate of microplastic generation at all time points and had reached a cumulative release of microplastics at 475 particles/cm^2 by the 70th day of UV aging. The microplastic formation for the other treatments decreased in the order of oxodegradable mulch film, PE white mulch film, and PE black mulch film with cumulative quantities of microplastics released at 265, 163, and 147 particles/cm^2, respectively.

The analysis of the particle size distributions of released microplastics led to a deeper insight into the behavior and potential hazard of the different types of mulch films. For all of the four types of mulch films, the majority of the released plastic particles ranged between 20 μm and 100 μm in size (Figs. 4 and 5). Previous studies have reported that microplastics in this range of particle sizes could be ingested and accumulated in soil animals, such as earthworms (Huerta Lwanga et al., 2017) and collembola (Maaß et al., 2017), thereby causing significant damaging effects on their growth, behavior, and survival rates. In addition, microplastics of this size range can accumulate around plant root hairs, thereby blocking the exchanges and adsorption of water or nutrients by plant cells (Bosker et al., 2019; Li et al., 2020), thus resulting in obvious oxidative damage, decreasing seed germination, and inhibiting plant growth (Qi et al., 2018). Moreover, with greater surface area-to-volume ratios, these smaller sized microplastics represent much more serious indirect ecosystem pollutants because of their high adsorption capacities and potential to transport toxic chemical or biochemical species (Chae and An, 2018). With the reduction of the particle sizes of microplastics, the chemical toxicities and biological availability of microplastics could be increased (de Souza Machado et al., 2018; Liu et al., 2021; Stubbins et al., 2021).

As shown in Figs. 4 and 5, the microplastics from the oxodegradable mulch films were more concentrated at the size range of 0.20 μm to 0.20 mm, which were smaller than the microplastics from the three other types of mulch films. This phenomenon could be due to the presence and uniform distribution of prooxidants in the oxodegradable mulch films that resulted in more evenly distributed crack propagations on the surface

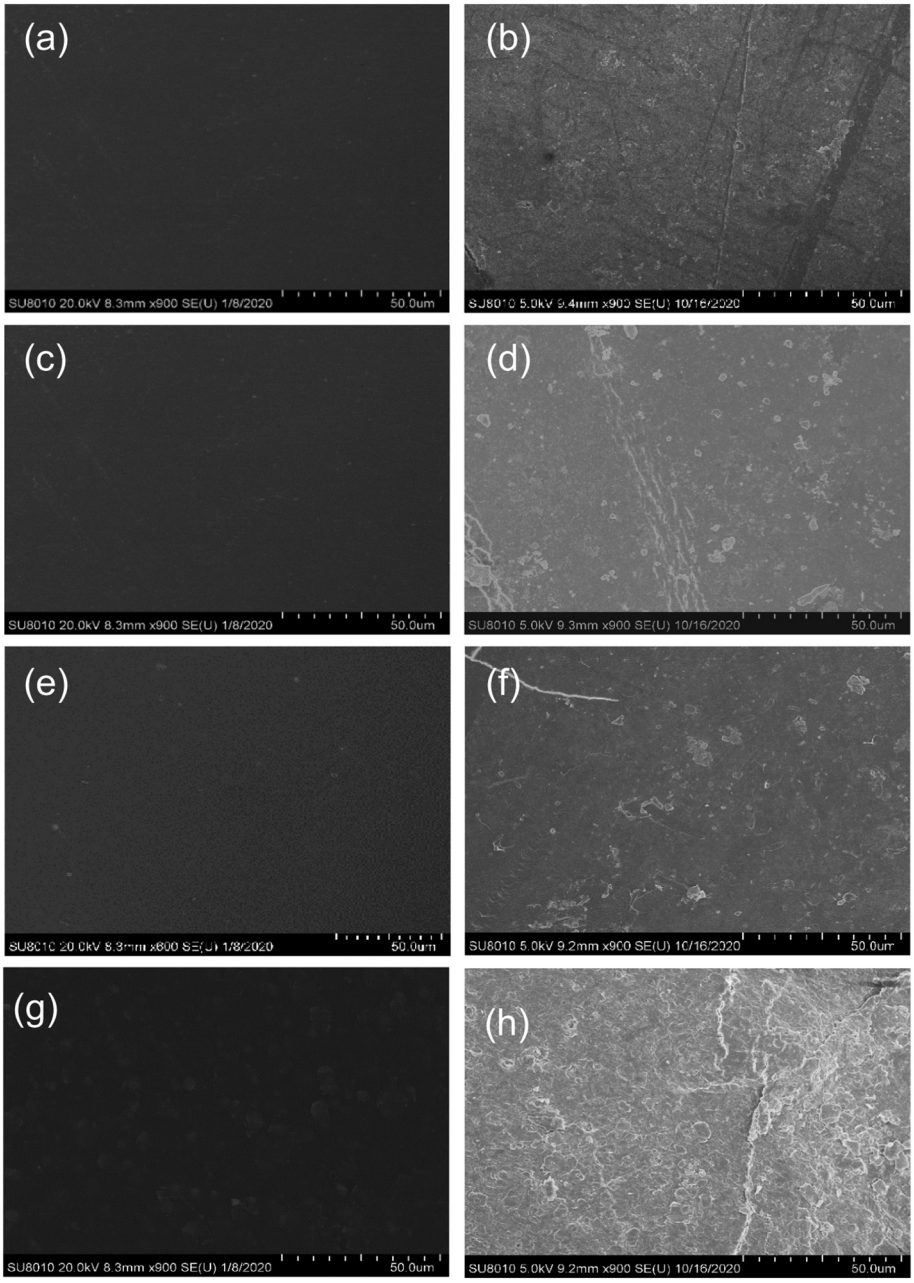

Fig. 3. SEM micrograph of mulch films aged for 0 d (a, c, e, g) and 70 d (b, d, f, h). (a, b) PE white, (c, d) PE black, (e, f) oxo degradable, and (g, h) biodegradable mulch films. The averaged UV intensity at the surface of the film debris is 8.10 μmol·m^{-2}·s^{-1}.

of this plastic mulch film, thus leading to the formation of smaller sized fragments. Furthermore, with the prolongation of UV irradiation period, a proportional increase in smaller sized microplastics, particularly for biodegradable mulch films, was observed. However, biodegradable mulch films are mainly constructed by polyesters, wherein the molecular structures are less compact and molecular bonds are less obstinate, thereby making it more accessible and sensitive to secondary degradations and final mineralization. Indeed, approximately 80% of carbon atoms for biodegradable materials (i.e., cellulose) can be converted into CO_2 in 90 days. However, the mineralize level for polyethylene and oxodegradable polyethylene in the same time course are very limited (Portillo et al., 2016). Overall, considering that biodegradable materials can be finally mineralized in a reasonable period of time, the implications of large amounts of small-sized microplastics from oxodegradable and non-degradable mulch films require more critical attention.

Table 2
Surface crystallinity for original and aged mulch films.

Aging time	Crystallinity (%)			
	PE white	PE black	Oxo-film	Bio-film
0 days	30.06	30.05	26.79	58.94
70 days	33.56	30.26	32.84	73.77

3.4. Reciprocal kinetics for microplastic emission

A critical point for understanding the patterns and rates of microplastic generation is to establish the kinetic models to build the quantitative linkage between the release of microplastics to key environmental factors

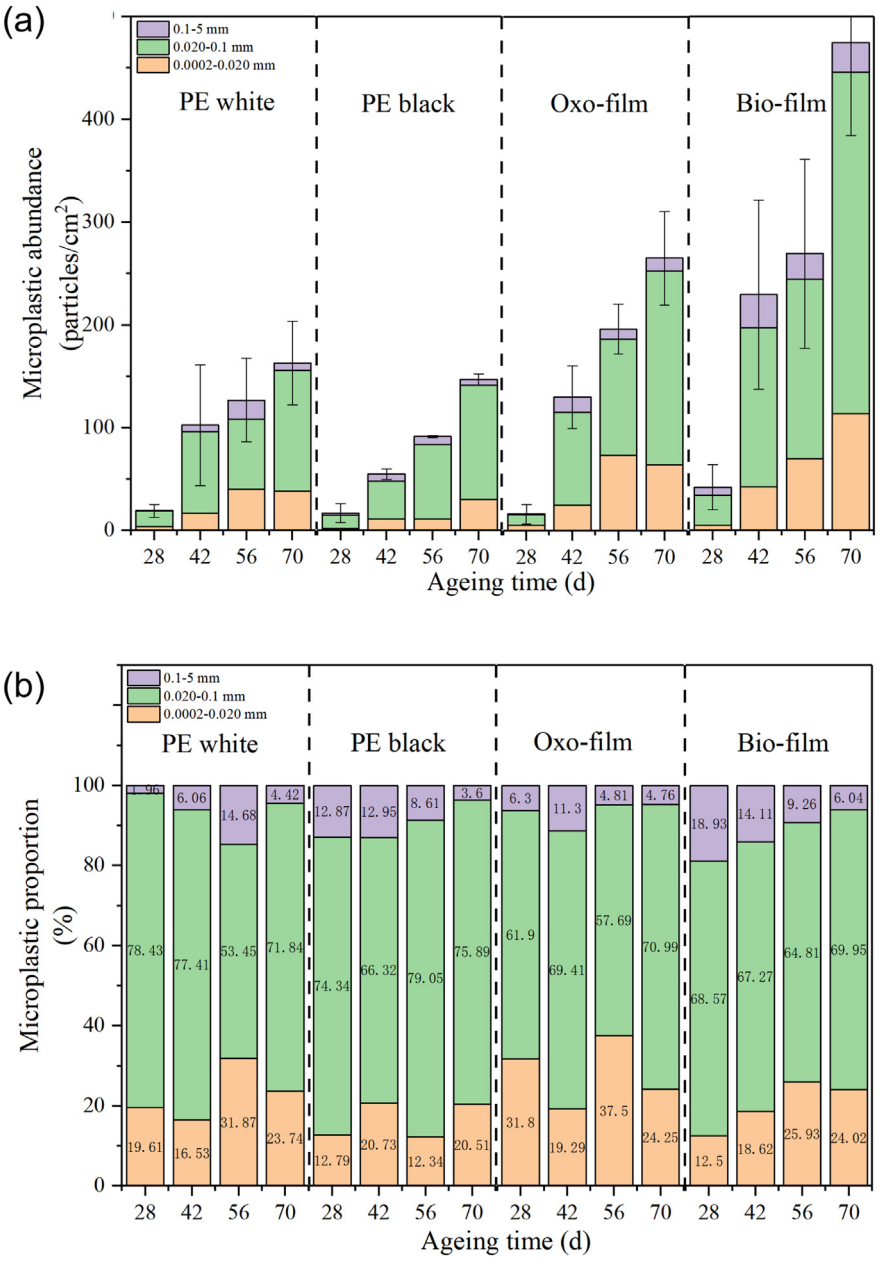

Fig. 4. Microplastic generation from different mulch films exposed to various periods of UV radiation. The averaged UV intensity at the surface of the film debris is 8.10 μmol·m^{-2}·s^{-1}. Bars = ±standard error, n = 3.

that control degradation (e.g., UV light). The well-known reciprocal principle and its generalized version, the Schwarzschild's law, has been widely used as the fundamental basis for predicting the effects of UV light on degradation processes (Chin et al., 2005; Croll, 2019; Fairbrother et al., 2019; Lyu et al., 2018). Two basic conditions have to be satisfied for reactions that follows Schwarzschild's principle: (i) the photoreaction plays a rate-determining role; and (ii) the radiant flux is at normal intensity, that is, neither too high nor too low (Martin et al., 2003). Referring to the emission of microplastics at simulated natural photo conditions, which is critically dependent on the photon scissions of macromolecular chains in the plastic materials, and the emission quantity of microplastics that were cumulatively increased with prolonged UV irradiation (Figs. 4a and 5), it is strongly suggested that microplastic emissions are possible UV responses that follow the Schwarzschild's law.

To assess whether the Schwarzschild's law is obeyed, we took advantage of the Hahm graphical method by taking logarithms on both sides of Schwarzschild's equation. As shown in Fig. 6, linear relationship between the logarithm of photo response vs the logarithm of light intensity for each of the mulch films was determined, implying that the microplastic generation of the different types of mulch films were all proportional to photo irradiation and therefore well agreed with the Schwarzschild's principle. The calculated *p*-coefficient factor is rated at 1.6309 for PE black mulch film, 1.7297 for PE white mulch film, 1.8778 for oxodegradable mulch film, and 2.0502 for biodegradable mulch film, with R^2 ranging between 0.9519 and 0.9850, respectively. The parameters of the microplastic generation kinetic models for the different types of mulch films are summarized in Table 3.

In previous studies, the Schwarzschild's law has been widely proven to exhibit excellent performance in interpreting and predicting plastic deterioration behaviors, such as chemical changes, yellowish coloring, or decreases in mechanical strength upon UV radiation (Diepens and Gijsman, 2009; Martin et al., 2003; Fairbrother et al., 2019), especially when photochemical reaction controls the outcome of the environmental

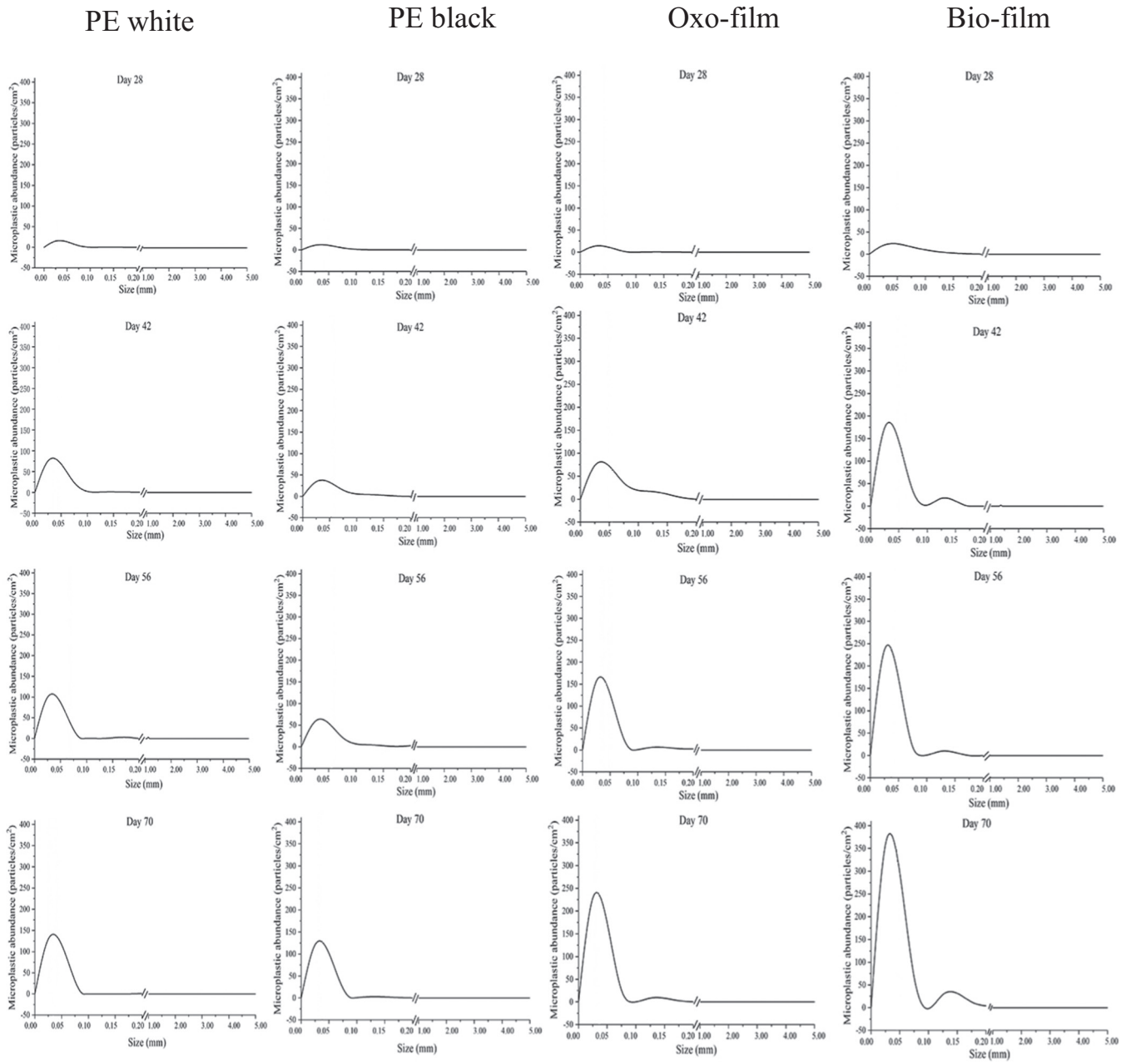

Fig. 5. Size distribution of microplastics from different mulch films following different periods of UV exposure. The averaged UV intensity at the surface of the film debris is 8.10 μmol·m^{-2}·s^{-1}.

exposure. Reports on the Schwarzchild's coefficient factor *p* have ranged from 0.04 to 1.85, in accordance to the different types of materials, light sources, and/or photochemical responses (Martin et al., 2003). However, this work is the first study for the evaluation of the Schwarzchild's law on the generation of microplastics upon photo-oxidation.

3.5. Implications from the Schwarzchild's kinetic model

Here, the coefficient factor *p* ranged between 1.6309 and 2.0502 (Table 3). The emission curves of microplastics are shown in Fig. 7, demonstrating that the quantity of microplastics generated from different types of plastic mulch films increases exponentially with the increased exposure to UV irradiation. According to the formula, significantly higher amounts of microplastics would be released from the oxodegradable and biodegradable mulch films compared with the PE white or black mulch films at the same photo irradiance. Also, the differences in the quantities of microplastics released by various plastic mulch films will be further widened with prolonged UV aging processes.

The reciprocal and Schwarzchild's law have also been proven to be powerful tools in simulating and predicting the property changes of polymeric materials during photodegradation. Thus, they are widely used in material service life prediction and comparison. As demonstrated in the reciprocal law, the photo responses of a material is only dependent on the cumulative quantity of the efficient radiation energy (neither too high that may cause corruptions to the material, nor too low that is incapable of breaking the molecular bond), instead of the radiation intensity, pattern, or weathering time separately. Therefore, very importantly, previous studies reported that although the irradiance of natural light sources change constantly with daily and seasonal variations, weathering results can only be expressed and predicted by comparing the accumulated irradiation dosage

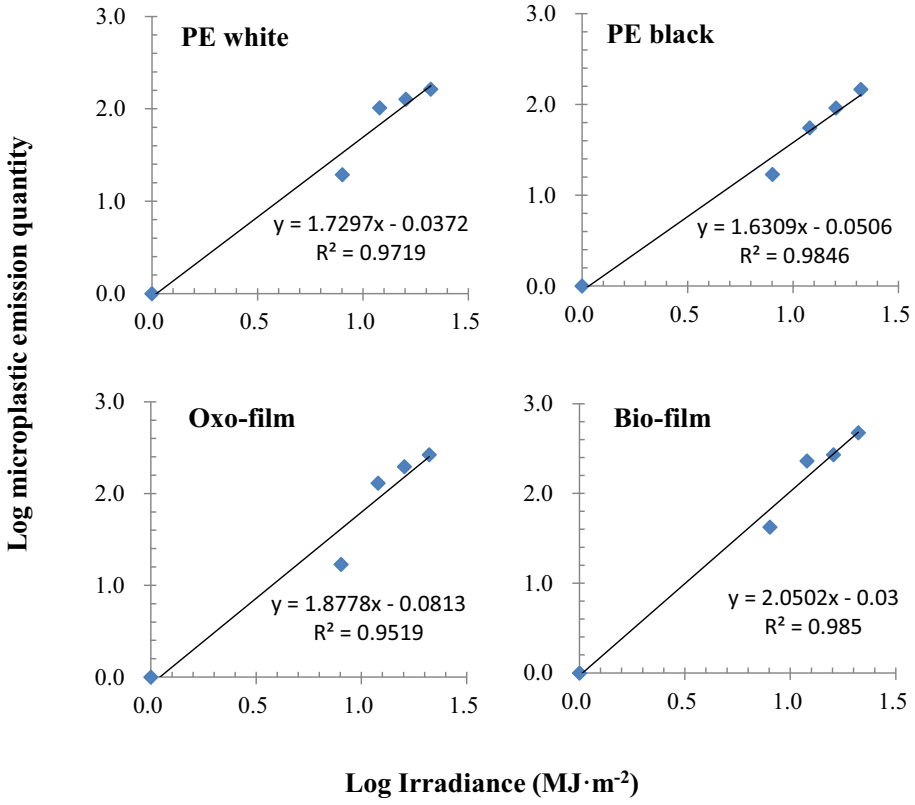

Fig. 6. Halm's graphical logarithm plot for PE white, PE black, oxo degradable, and biodegradable mulch films.

using the validated reciprocal principle. Moreover, the reciprocal and Schwarzchild's law suggest that the degrees of photodegradation are proportional to the cumulative irradiant degrees, that is, if the irradiance increases, the extent of photo damages rises exponentially. Based on this, we extended the emission curves of microplastics to as long as 200 days and predicted an emission quantity of microplastics at 4603, 2236, 1218, 818 particles/cm^2 for biodegradable, oxodegradable, and white and black non-degradable mulch films, respectively (Fig. S2). This represents a huge source of microplastics within agricultural soils with implications for soil and crop health, as well as transfers to the aquatic environment.

Our SEM (Fig. 2) and XRD (Table 2) results suggested the concurrent increase in the crystallinity and surface erosion (surface-volume ratio) of the mulch films upon UV irradiation, in which two factors cause antagonistic influences on the accessibility of the materials to photo degradation and the kinetics of microplastic formation. To account for this, the Gurney–Mott model could be applied in future studies. The principle of the Gurney–Mott model is that while photochemical changes are complex and vary among materials, photo-physical processes (e.g., photon absorptions) are identical in all materials and always happens prior to photochemical events (Croll, 2019; Francois-Heude et al., 2014; Gurney and Mott, 1938; Martin et al., 2003). Changes in the crystallinity and surface–volume ratio, which can be translated as the sensitivity or accessibility of the molecular chains to photo radiation, can be accounted for in the Gurney–Mott model. Further investigations and revisions to the kinetics of microplastic formation using the Gurney–Mott principle models may lead to a more comprehensive view on the mechanisms and kinetics of microplastic emission.

Table 3
Kinetic model on microplastic emission by Schwarzchild's law.

Mulch films	Micro plastic emission	
	p	R^2
PE white	1.7297	0.9719
PE black	1.6309	0.9846
Oxo-film	1.8778	0.9519
Bio-film	2.0502	0.9850

4. Conclusion

Plastic film mulching has significantly contributed to the agricultural development in China. However, large emissions of macro- and microplastic debris from mulch films to the environment are increasingly recognized as serious pollutants. In this study, we made a quantitative investigation on the formation of microplastic from different types of mulch films. A dose-dependent relationship of microplastic generation from mulch films upon UV irradiation that follows strictly to the Schwarzschild's law was demonstrated. The calculated coefficient factor *p* for Bio-, Oxo-, PE white, and PE black mulch films are rated at 2.0502, 1.8778, 1.7297, and 1.6309, respectively. At a cumulative UV irradiation of 2.1 MJ/m^2 at soil surface, which resembles a cumulative irradiance level of 70 days of natural summer solar light in the North of China (Zhu et al., 2021), the average quantity of microplastics released from biodegradable, oxodegradable, and white and black non-degradable mulch films at the size ranges of 0.02–0.10 mm are 475, 266, 163, and 147 particles/cm^2, respectively. To our knowledge, this study is the first quantitative interpretation on the kinetics of microplastic generation in reference to the Schwarzschild's principle. Our results alarm for a huge source of microplastic pollution to agricultural soil by plastic film mulching. Further investigations on the retention time and final state of the microplastics from different types of mulch films will be needed for a more complete evaluation of the environmental influences. Moreover, more complexed environmental factors, such as the photon absorption efficiency of the aged materials, should be considered in future studies.

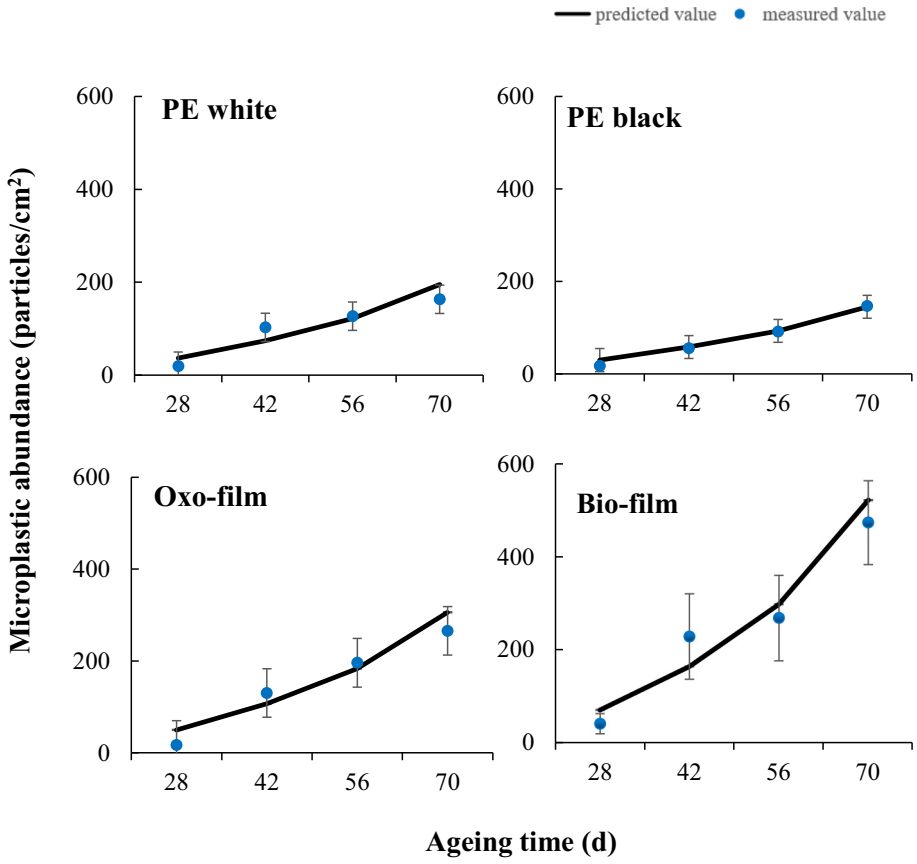

Fig. 7. Microplastic emission model plot for the different types of mulch films. Detected data of microplastic generation (blue dots) and predicted emission curve of microplastics upon UV irradiation (black curve) at averaged UV intensity of 8.10 μmol·m^{-2}·s^{-1} at the surface of the films. Bars = ±standard error, n = 3.

CRediT authorship contribution statement

Yang Yang: Methodology, Investigation, Data curation, Validation, Writing - original draft; **Zhen Li:** Conceptualization, Methodology, Writing - original draft, Writing - review & editing; **Changrong Yan:** Supervision, Writing - review & editing; **Dave Chadwick:** Writing - review & editing; **Davey L. Jones:** Writing - review & editing; **Enke Liu:** Methodology; **Qin Liu:** Data curation; **Runhao Bai:** Data curation; **Wenqing He:** Conceptualization, Methodology, Funding acquisition, Project administration, Supervision, Writing - review & editing.

Declaration of competing interest

The authors declare that they have no known competing financial interests or personal relationships that could have appeared to influence the work reported in this paper.

Acknowledgements

We are grateful for the grants of Newton UK-China Agritech Challenge the Zero-Waste Agricultural Mulch Films for Crops in China project (2017YFE0121900), National Natural Science Foundation of China (No. 42007394), Government of Inner Mongolia Autonomous Region Science and Technology Plan Project (2021GG0063), Xinjiang Production and Construction Corps Key R&D Program Project (2021AB007), National Natural Science Foundation of China (No. 42007312), Central Public-interest Scientific Institution Basal Research Fund, CAFS (No. BSRF202001), Key R & D Project of Hainan Province (SQ2020XDNY0113).

Appendix A. Supplementary data

Supplementary data to this article can be found online at https://doi.org/10.1016/j.scitotenv.2021.152572.

References

Albertsson, A.C., Hakkarainen, M., 2017. Designed to degrade. Science 58 (6365), 872–873.
Ammala, A., Bateman, S., Dean, K., Petinakis, E., Sangwan, P., Wong, S., Yuan, Q., Yu, L., Patrick, C., Leong, K.H., 2011. An overview of degradable and biodegradable polyolefins. Prog. Polym. Sci. 36, 1015–1049.
Bhagat, J., Zang, L., Nishimura, N., Shimada, Y., 2020. Zebrafish: an emerging model to study microplastic and nanoplastic toxicity. Sci. Total Environ. 728 (2), 138707.
Bigger, S.W., Scheirs, J., Delatycki, O., 1992. Effect of light intensity on the photooxidation kinetics of high-density polyethylene. J. Polym. Sci. 30, 2277–2280.
Bosker, T., Bouwman, L.J., Brun, N.R., Behrens, P., Vijver, M.G., 2019. Microplastics accumulate on pores in seed capsule and delay germination and root growth of the terrestrial vascular plant Lepidium sativum. Chemosphere 226, 774–781.
Briassoulis, D., Babou, E., Hiskakis, M., Kyrikou, I., 2015a. Analysis of long-term degradation behaviour of polyethylene mulching films with pro-oxidants under real cultivation and soil burial conditions. Environ. Sci. Pollut. Res. 22, 2584–2598.
Briassoulis, D., Babou, E., Hiskakis, M., Kyrikou, I., 2015b. Degradation in soil behavior of artificially aged polyethylene films with pro-oxidants. J. Appl. Polym. Sci. 42289.
Cai, L., Wang, J., Peng, J., Wu, Z., Tan, X., 2018. Observation of the degradation of three types of plastic pellets exposed to UV irradiation in three different environments. Sci. Total Environ. 628, 740–747.
Chae, Y., An, Y.J., 2018. Current research trends on plastic pollution and ecological impacts on the soil ecosystem: a review. Environ. Pollut. 240, 387–395.
Chen, X., Xu, M., Yuan, L., Huang, G., Chen, X., Shi, W., 2021. Degradation degree analysis of environmental microplastics by micro FT-IR imaging technology. Chemosphere 274, 129779.
Chin, J., Nguyen, T., Byrd, E., Martin, J., 2005. Validation of the reciprocity law for coating photodegradation. JCT Res. 2 (7), 499–508.
China Agriculture Yearbook, 2019. China Agriculture Yearbook. China Agriculture Press, Beijing.

Croll, S.G., 2019. Reciprocity in weathering exposure and the kinetics of property degradation. Prog. Org. Coat. 127, 140–150.
de Souza Machado, A.A., Lau, C.W., Kloas, W., Bergmann, J., Bachelier, J.B., Faltin, E., Becker, R., Gorlich, A.S., Rilling, M.C., 2019. Microplastics can change soil properties and affect plant performance. Environ. Sci. Technol. 53, 6044–6052.
de Souza Machado, A.A., Kloas, W., Zarfl, C., Hempel, S., Rillig, M.C., 2018. Microplastics as an emerging threat to terrestrial ecosystems. Glob. Chang. Biol. 24, 1405–1416.
Diepens, M., Gijsman, P., 2009. Influence of light intensity on the photodegradation of bisphenol a polycarbonate. Polym. Degrad. Stab. 94 (1), 34–38.
Ding, W., Li, Z., Qi, R., Jones, D.L., Liu, C., Liu, Q., Yan, C., 2021. Effect thresholds for the earthworm eisenia fetida: toxicity comparison between conventional and biodegradable microplastics. Sci. Total Environ. 781 (8), 146884.
Eriksen, M., Lebreton, L.C., Carson, H.S., Thiel, M., Moore, C.J., Borerro, J.C., Galgani, F., Ryan, P.G., Reisser, J., 2014. Plastic pollution in the world's oceans: more than 5 trillion plastic pieces weighing over 250,000 tons afloat at sea. PLoS One 9, 0111913.
Fairbrother, A., Hsueh, H.C., Kim, J.H., Jacobs, D., Perry, L., Goodwin, D., White, C., Watson, S., Sung, L.P., 2019. Temperature and light intensity effects on photodegradation of high-density polyethylene. Polym. Degrad. Stab. 165, 153–160.
Francois-Heude, A., Richaud, E., Desnoux, E., Colin, X., 2014. Influence of temperature, UV-light wavelength and intensity on polypropylene photothermal oxidation. Polym. Degrad. Stab. 100, 10–20.
Gao, H., Yan, C., Liu, Q., Ding, W., Chen, B., Li, Z., 2019. Effect of plastic mulching and plastic residue on agricultural production: a meta-analysis. Sci. Total Environ. 651, 484–492.
Gurney, R.W., Mott, N.F., 1938. The theory of the photolysis of silver bromide and the photographic latent image. Proc. R. Soc. Lond. A 64, 151–167.
He, D., Luo, Y., Lu, S., Liu, M., Song, Y., Lei, L., 2018. Microplastics in soils: analytical methods, pollution characteristics and ecological risks. TrAC Trends Anal. Chem. 109, 163–172.
Horton, A.A., Walton, A., Spurgeon, D.J., Lahive, E., Svendsen, C., 2017. Microplastics in freshwater and terrestrial environments: evaluating the current understanding to identify the knowledge gaps and future research priorities. Sci. Total Environ. 586, 127–141.
Hsu, Y.C., Weir, M.P., Truss, R.W., Garvey, C.J., Nicholson, T.M., Halley, P.J., 2012. A fundamental study on photo-oxidative degradation of linear low density polyethylene films at embrittlement. Polymer 53, 2385–2393.
Huang, Y., Liu, Q., Jia, W., Yan, C., Wang, J., 2020. Agricultural plastic mulching as a source of microplastics in the terrestrial environment. Environ. Pollut. 260, 114096.
Huerta Lwanga, E., Vega, J.M., Quej, V.K., Chi, J.A., Cid, L.S., Chi, C., Segura, G.E., Gertsen, H., Salanki, T., Ploeg, M., Koelmans, A.A., Geissen, V., 2017. Field evidence for transfer of plastic debris along a terrestrial food chain. Sci. Rep. 7, 14071.
Iniguez, M.E., Conesa, J.A., Fullana, A., 2018. Recyclability of four types of plastics exposed to UV irradiation in a marine environment. Waste Manag. 79, 339–345.
Julienne, F., Lagarde, F., Delorme, N., 2019. Influence of the crystalline structure on the fragmentation of weathered polyolefines. Polym. Degrad. Stab. 170, 109012.
Kasirajan, S., Ngouajio, M., 2012. Polyethylene and biodegradable mulches for agricultural applications: a review. Agron. Sustain. Dev. 32, 501–529.
Laycock, B., Nikolic, M., Colwell, J.M., Gauthier, E., Halley, P., Bottle, S., George, G., 2017. Lifetime prediction of biodegradable polymers. Prog. Polym. Sci. 17, 144–189.
Lambert, S., Wagner, M., 2016. Characterisation of nanoplastics during the degradation of polystyrene. Chemosphere 145, 265–268.
Lehner, R., Weder, C., Petri, F.A., Rothen, R.B., 2019. Emergence of nanoplastic in the environment and possible impact on human health. Environ. Sci. Technol. 53, 1748–1765.
Li, L., Luo, Y., Li, R., Zhou, Q., Peijnenburg, W., Yin, N., Yang, J., Tu, C., Zhang, Y., 2020. Effective uptake of submicrometer plastics by crop plants via a crack-entry mode. Nat. Sustain. 3, 929–937.
Li, Z., Liu, Q., He, W., Yan, C., 2018. Contamination hazard of plastic mulching residues in China. Plasticulture 139, 64–67.
Li, Z., He, W., Liu, E., Zhou, J., Liu, Q., Yan, C., 2019. A review on polyethylene mulch film degradation. J. Agro-Environ. Sci. 38 (2), 268–275.
Liu, E.K., He, W.Q., Yan, C.R., 2014. White revolution to white pollution: agricultural plastic film mulch in China. Environ. Res. Let. 9, 091001.
Liu, M., Lu, S., Song, Y., Lei, L., Hu, J., Lv, W., Zhou, W., Cao, C., Shi, H., Yang, X., He, D., 2018. Microplastic and mesoplastic pollution in farmland soils in suburbs of Shanghai, China. Environ. Pollut. 242, 855–862.
Liu, Y., Shao, H., Liu, J., Cao, R., Shang, E., Liu, S., Li, Y., 2021. Transport and transformation of microplastics and nanoplastics in the soil environment: a critical review. Soil Use Manag. 37, 224–242.
Lyu, Y., Kim, J.H., Gu, X., 2018. Developing methodology for service life prediction of PV materials: quantitative effects of light intensity and wavelength on discoloration of a glass/EVA/PPE laminate. Sol. Energy 174, 515–526.
Maaß, S., Daphi, D., Lehmann, A., Rillig, M.C., 2017. Transport of microplastics by two collembolan species. Environ. Pollut. 225, 456–459.
MacLeod, M., Arp, H.P.H., Tekman, M.B., Jahnke, A., 2021. The global threat from plastic pollution. Science 373, 61–65.
Martin, J.W., Chin, J.W., Nguyen, T., 2003. Reciprocity law experiments in polymeric photodegradation: a critical review. Prog. Org. Coat. 47, 292–311.
Portillo, F., Yashchuk, O., Hermida, E., 2016. Evaluation of the rate of abiotic and biotic degradation of oxo-degradable polyethylene. Polym. Test. 53, 58–69.
Qi, R., Jones, D.L., Li, Z., Liu, Q., Yan, C., 2020. Behavior of microplastics and plastic film residues in the soil environment: a critical review. Sci. Total Environ. 703, 1–12.
Qi, Y., Yang, X., Mejia, P.A., Huerta Lwanga, E., Beriot, N., Gertsen, H., Garbeva, P., Geissen, V., 2018. Macro- and micro-plastics in soil-plant system: effects of plastic mulch film residues on wheat (Triticum aestivum) growth. Sci. Total Environ. 645, 1048–1056.
Rillig, M.C., 2012. Microplastic in terrestrial ecosystems and the soil? Environ. Sci. Technol. 46 (12), 6453–6454.
Rillig, M.C., Ingraffia, R., de Souza Machado, A.A., 2017. Microplastic incorporation into soil in agroecosystems. Front. Plant Sci. 8, 1805.
Rudnik, E., Briassoulis, D., 2011. Comparative biodegradation in soil behaviour of two biodegradable polymers based on renewable resources. J. Polym. Environ. 19, 18–39.
Somersall, A.C., Guillet, J.E., 1985. Computer modeling studies of polymer photooxidation and stabilization. Polym. Stab. Degrad. 16, 221–234.
Steinmetz, Z., Wollmann, C., Schaefer, M., Buchmann, C., David, J., Troger, J., Munoz, K., Fror, O., Schaumann, G.E., 2016. Plastic mulching in agriculture. Trading short-term agronomic benefits for long-term soil degradation? Sci. Total Environ. 550, 690–705.
Stubbins, A., Law, K.L., Munoz, S.E., Bianchi, T.S., Zhu, L., 2021. Plastics in the earth system. Science 373, 51–55.
Sun, D., Li, H., Wang, E., He, W., Hao, W., Yan, C., Li, Y., Mei, X., Zhang, Y., Sun, Z., Jia, Z., Zhou, H., Fan, T., Zhang, X., Liu, Q., Wang, F., Zhang, C., Shen, J., Wang, Q., Zhang, F., 2020. An overview of the use of plastic-film mulching in China to increase crop yield and water-use efficiency. Nat. Sci. Rev. 7, 1523–1526.
Thompson, R.C., Swan, S.H., Moore, C.J., vom Saal, F.S., 2009. Our plastic age. Philos. Trans. R. Soc. Lond. Ser. B Biol. Sci. 364, 1973–1976.
Uheida, A., Mejia, H.G., Abdel, R.M., Hamd, W., Dutta, J., 2021. Visible light photocatalytic degradation of polypropylene microplastics in a continuous water flow system. J. Hazard. Mater. 406, 124299.
Yan, C.R., He, W.Q., Liu, S., Cao, S.L., 2015. Application of Mulch Films and Prevention of its Residual Pollution in China. China Sci. Publication, Beijing, p. 279.
Zhang, K., Hamidian, A.H., Tubic, A., Zhang, Y., Fang, J.K.H., Wu, C., Lam, P.K.S., 2021. Undertanding plastic degradation and microplastic formation in the environment: a review. Environ. Pollut. 274, 116554.
Zhao, X., Li, Z., Chen, Y., Shi, L., Zhu, Y., 2006. Solid-phase photocatalytic degradation of polyethylene plastic under UV and solar light irradiation. J. Mol. Catal. A Chem. 268, 101–106.
Zhu, B., Sun, S., Li, Y., Zhang, H., Jing, L., Wang, L., Cao, W., 2021. Characteristics of ultraviolet radiation and global radiation in alpine desert: a case of hulun buir Sandy land. J. Desert Res. 41 (1), 111–118.
Zhou, B.Y., Wang, J.Q., Zhang, H.B., Shi, H.H., Fei, Y.F., Huang, S.Y., Tong, Y.Z., Wen, D.S., Luo, Y.M., Barcelo, D., 2020. Microplastics in agricultural soils on the coastal plain of Hangzhou Bay, East China: multiple sources other than plastic mulching film. J. Hazard. Mater. 388, 121814.
Zhu, K., Jia, H., Sun, Y., Dai, Y., Zhang, C., Guo, X., Wang, T., Zhu, L., 2020. Long-term phototransformation of microplastics under simulated sunlight irradiation in aquatic environments: roles of reactive oxygen species. Water Res. 173, 115564.
Zumstein, M.T., Schintlmeister, A., Nelson, T.F., Baumgartner, R., Woebken, D., Wagner, M., Kohler, H.P.E., McNeill, K., Sander, M., 2018. Biodegradation of synthetic polymers in soils: tracking carbon into CO2 and microbial biomass. Sci. Adv. 4, 9024.